

Supporting Information for Towards Microwave Imaging of Cells

Mehmet Kelleci^{1,*}, Hande Aydoğmuş^{1,*}, Levent Aslanbaş^{1,*}, Selçuk Oğuz Erbil^{1,*},
M. Selim Hanay^{1,2,†}

¹Department of Mechanical Engineering;
²National Nanotechnology Research Center (UNAM),
Bilkent University, Ankara, 06800 Turkey

S1. Two Mode PLL

The measurement system based on microwave interferometer circuit described elsewhere.³ To track the resonance frequency in real time, we used a closed loop system with a PI controller. To transduce two modes simultaneously, we combined RF signals with power splitters. To avoid cross-talk, we mixed down the sensor output to different lock-in frequencies⁴. A schematic of the overall circuitry is shown in Main Text Figure 2. The performance for the sensors are characterized by Allan Deviation. In Figure S7 on the next page, the response time for each PLL is shown to be on the order of 0.4 seconds (Figure S7a and S7b). In these control runs, the frequency fluctuations are shown and the associated Allan deviations are obtained (Figure S7). The Allan Deviation for the first mode is $1.5 \cdot 10^{-8}$ and the second mode is $1.8 \cdot 10^{-8}$ for 400 ms timescale which is the response time of the PLL.

* These authors contributed equally to this work.

† Corresponding author, e-mail: selimhanay@bilkent.edu.tr

Supporting Information for Towards Microwave Imaging of Cells

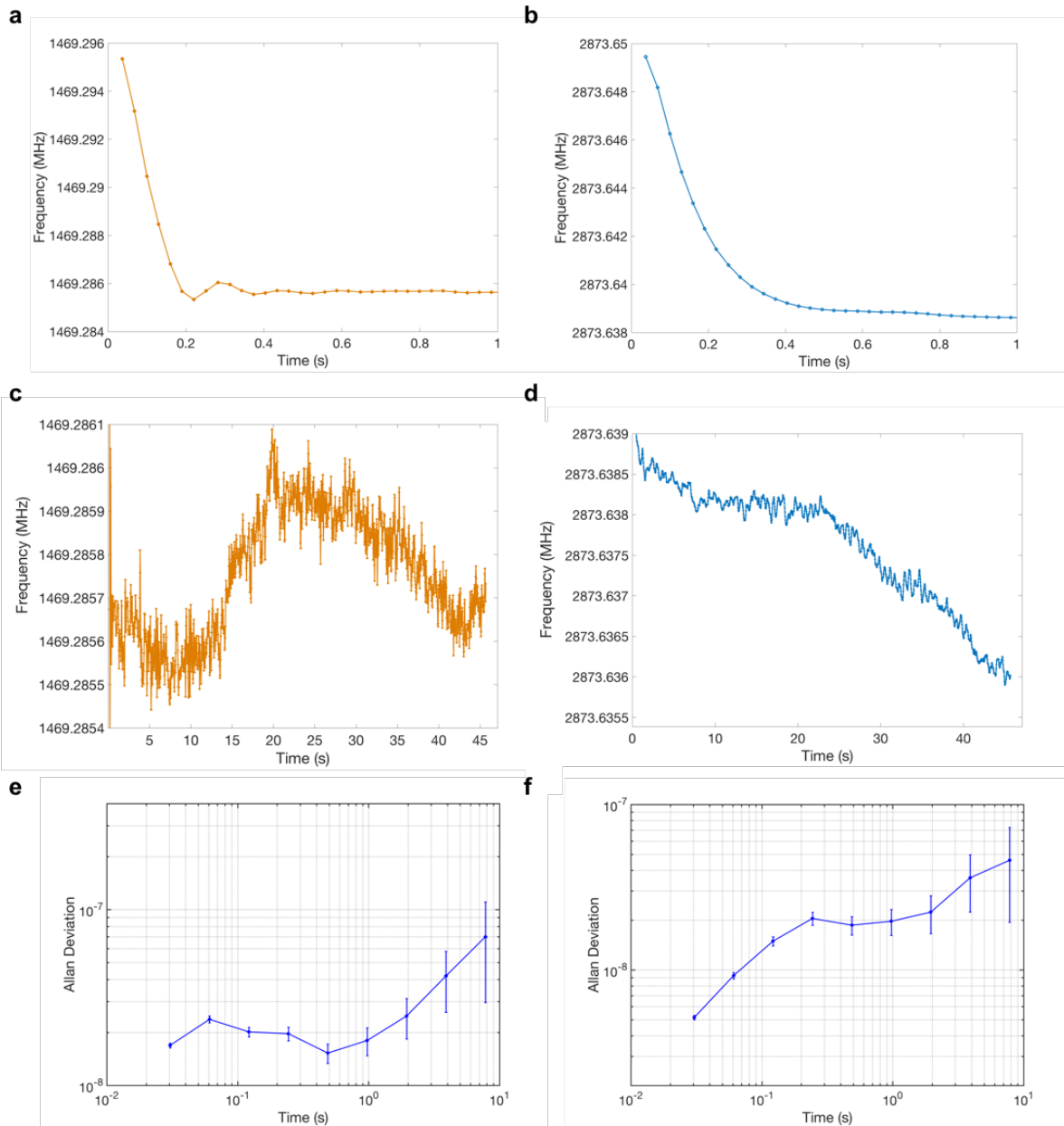


Figure 1: Control run for measuring the frequency stability of both modes. In the experiments, the response time is measured by starting the PLLs slightly away from the actual resonance values. The PLL then brings the drive frequency back to microwave sensor's resonance frequency for the first (a) and the second (b) mode. On both cases, the frequency stabilizes within 400 ms after the run is started. In (c) and (d), the rest of the PLL run is shown. The calculated Allan Deviations are shown in (e) for the first mode and (f) for the second mode.

S2. Position Histogram for HeLa and MDA Cells

Two different set of channels were used so that HeLa and MDA cells flow through different locations of the sensor. The scatter plot for the frequency 1 – frequency 2 planes and position histograms are shown below. The mean position for the MDA cells is $\langle x \rangle = 0.426$ and the standard deviation $\sigma_x = 0.020$ which is quite sharp – possibly because only one channel carries most of the flow. Indeed, the position data for MDA is consistent with a flow through a channel located at 30.54 mm away from the edge of a 69.35 mm long device ($\frac{30.54}{69.35} = 0.440$). On the other hand, the mean position for the HeLa data, $\langle x \rangle = 0.325$ with a relatively large standard deviation in position distribution: $\sigma_x = 0.059$. This large value of standard deviation suggests that two channels may have similar contributions for the flow of the cells. Indeed, the combined effect of two channels located at 20.39 mm and 24.87 mm away from the edges correspond to normalized positions of 0.294 and 0.359 , with an average value of 0.326 which is very close to the measured mean position (0.325).

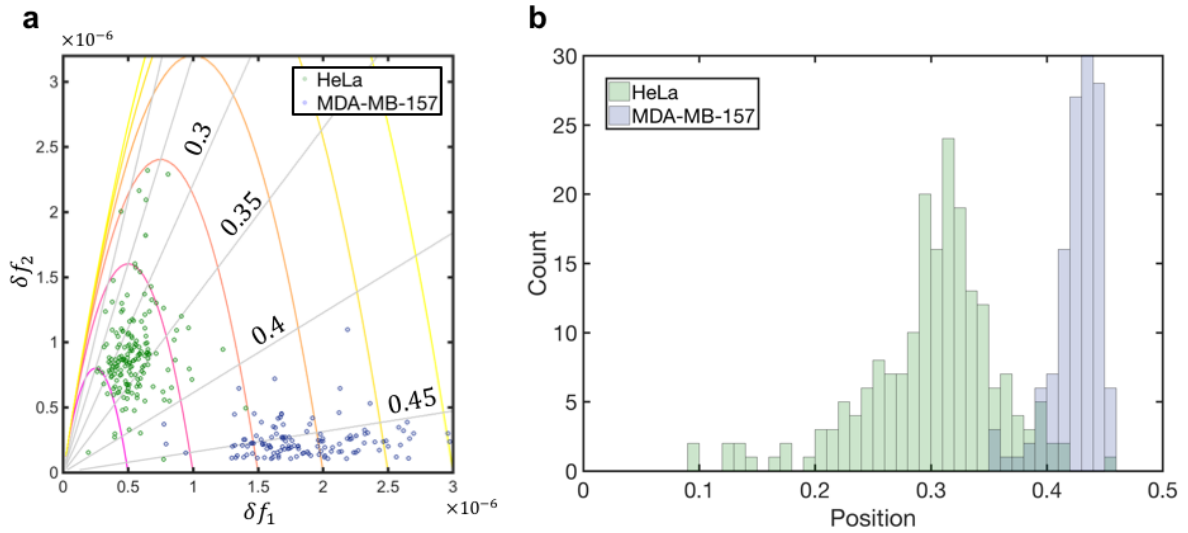


Figure 2: (a) Scatter plate in the df_1 - df_2 plane, and (b) position histogram for the two cell lines used in the experiments.

S3. Position and Electrical Volume of Droplets

To check if the value for the electrical volume agrees with the theory, we have applied Maxwell-Garnett approach, $\epsilon_{MG} = \epsilon_h \left(1 + 3f \frac{\epsilon_i - \epsilon_h}{\epsilon_i + 2\epsilon_h} \right)$. Starting with the basic frequency shift equation:

$$\frac{\Delta f_n}{f_n} = - \frac{\int_{V_0} \Delta \epsilon(\mathbf{r}) E_n^2(\mathbf{r}) d^3 \mathbf{r}}{\int_{V_0} (\epsilon(\mathbf{r}) E_n^2 + \mu(\mathbf{r}) H_n^2) d^3 \mathbf{r}}$$

Supporting Information for
Towards Microwave Imaging of Cells

Here the denominator is over the entire device and the largest contribution comes from the PDMS part. On the other hand, the integral over the numerator has non-zero value only on the channel where the inclusion of a particle and exclusion of the corresponding fluid creates a change in permittivity $\Delta\epsilon$ which then can be calculated through Maxwell-Garnett approach. In this case:

$$\Delta\epsilon = \epsilon_{MG} - \epsilon_h = 3f\epsilon_h \frac{\epsilon_i - \epsilon_h}{\epsilon_i + 2\epsilon_h}$$

where ϵ_h is the permittivity of the excluded (host) material (oil for microdroplet experiments and cell media for cell experiments) and ϵ_i is the permittivity of the included material (water for microdroplet experiments and cell for cell experiments) and f is the filling ratio.

Taking the volume of the inclusion as the volume of the droplet ($f=1$ and the integral limit is only the volume of the particle) and disregarding the variation of Electrical field for clarity (in the discussion throughout the paper, we kept the modal variations in the electrical field and show how they can be exploited), we obtain:

$$\int \Delta\epsilon(\mathbf{r}) d^3\mathbf{r} = 3\epsilon_h \frac{\epsilon_i - \epsilon_h}{\epsilon_i + 2\epsilon_h} \int_{particle} d^3\mathbf{r} = 3\epsilon_h \frac{\epsilon_i - \epsilon_h}{\epsilon_i + 2\epsilon_h} V_{particle}$$

where $V_{particle}$ is the geometric volume of the particle. Note that the same conclusion could be reached if we set the integral limits around the channel: in this case the filling factor would have been $f = V_{particle}/V_{channel}$ and we obtain the same equation.

Therefore, the frequency shifts relate to electrical parameters as:

$$\frac{\Delta f_n}{f_n} = -\frac{1}{2\nu_{device}} 3\epsilon_h \frac{\epsilon_i - \epsilon_h}{\epsilon_i + 2\epsilon_h} V_{particle}$$

where ν_{device} is the electrical volume of the device. For water microdroplets in an oil medium, we have $\epsilon_i \gg \epsilon_h$, so for the denominator we have $\epsilon_i + 2\epsilon_h \approx \epsilon_i$. Moreover, the permittivities of oil and PDMS are close to each other, so $\frac{\nu_{device}}{\epsilon_h} \sim V_{device}$ and we can approximate the signal effect to be:

$$\left| \frac{\Delta f}{f_0} \right| \approx \frac{3}{2} \left(\frac{V_{droplet}}{V_{device}} \right)$$

For a more accurate estimate, we use $\epsilon_{water} = 78.3$, $\epsilon_{oil} = 2.5$ and we can calculate the signal magnitude:

$$\left| \frac{\Delta f}{f_0} \right| = 1.37 \left(\frac{V_{droplet}}{V_{device}} \right)$$

Supporting Information for
Towards Microwave Imaging of Cells

For the channel near the center, the first mode is much more responsive than the second mode and $\left|\frac{\Delta f}{f_0}\right| \sim 5 \cdot 10^{-5}$, therefore our technique predicts $\left(\frac{V_{droplet}}{V_{device}}\right) = 3.6 \cdot 10^{-5}$.

The droplet dimensions are $75\mu m \times 200\mu m \times 200\mu m$ as defined by the channel thickness and width, and the aspect ratio of droplets as observed under the microscope. The electrical volume of the device consists of the region under the microstrip line where a high density of almost uniform electric field exists as well as fringing fields through the air and the rest of the PDMS device. The volume of this region is: $1.3mm \times 69mm \times 970\mu m$ for the width and length of the microstripline and the thickness of PDMS. Therefore

$$\left(\frac{V_{droplet}}{V_{device}}\right) = \frac{75\mu m \times 200\mu m \times 200\mu m}{1.3mm \times 69mm \times 970\mu m} = 3.4 \cdot 10^{-5}$$

We see that the analysis using our technique and independently measured dimensions give very similar ratios for the volume ratio of droplets ($3.6 \cdot 10^{-5}$ vs. $3.4 \cdot 10^{-5}$) which endorses the analytic capability of our technique.

On the other hand, for cells in a water-based cell media, we have $\epsilon_{cell} \sim \epsilon_{media}$ and the term $\frac{3\epsilon_h}{\epsilon_i + 2\epsilon_h} \approx 1$ in the Maxwell-Garnett formula. So the relationship between frequency shifts and the electrical parameters become:

$$\left|\frac{\Delta f}{f}\right| \approx (\epsilon_{cell} - \epsilon_{media}) \frac{V_{cell}}{2v_{device}} = \frac{\Delta\epsilon V_{cell}}{2v_{device}} = \frac{1}{2} \frac{\Delta v_{cell}}{v_{device}}$$

where Δv_{cell} is the excess electrical volume of the cell: $\Delta v_{cell} = (\epsilon_{cell} - \epsilon_{media})V_{cell} = \Delta\epsilon V_{cell}$. The last formula is completely analogous to the formulas used in nanomechanical sensing literature where density of the particle replaces the permittivity of the particle. Therefore, the calculation of higher order moments can proceed by using the excess electrical volume of the cells.

S4. Permittivity Variation with Frequency

We note that the permittivity of the analyte and the device may change as a function of frequency, therefore the electrical volume defined for the particle (v) and for the mode (V) may include a slight dependency on the frequency. Moreover, deviations from ideal mode shapes and nonlinear response of the sensor introduces additional second order effects. To account for such effects, an empirical calibration factor α can be introduced – which mainly quantifies the ratio of the change in permittivity for the analyte over the change in effective permittivity for the device: $\alpha \equiv \frac{\Delta\epsilon(f_2) \epsilon_{eff}(f_1)}{\Delta\epsilon(f_1) \epsilon_{eff}(f_2)}$.

The value of α can be determined through independent characterization of system

components at different frequencies or could be fitted using the data, since channel locations are known. Incorporating the frequency-correction factor into the equation to yield:

$$x = \frac{1}{\pi} \arccos \left(\sqrt{\frac{\alpha \delta f_2}{4 \delta f_1}} \right)$$

In this experiment, the value of $\alpha = 1.6$ reconstructs the correct absolute position and electrical volume of the droplets used with reasonable accuracy. Channel positions and measurement results without the permittivity normalization (i.e. $\alpha = 1$) and with normalization are tabulated below. The standard deviation (1σ) in the position measurements are reported in parenthesis.

	Channel a	Channel b	Channel c	Channel d
Ideal	0.297	0.365	0.426	0.493
$\alpha = 1$	0.349 (0.005)	0.387 (0.005)	0.434 (0.009)	0.490 (0.011)
$\alpha = 1.6$	0.304 (0.007)	0.354 (0.006)	0.415 (0.009)	0.487 (0.015)

In figure 3a, measured locations are shown for the microdroplets and they agree well with the actual channel locations. In figure 3b, measured electrical volume emerges as a sharp peak: as expected from the near-uniform nature of droplet generation at $1.05 \pm 0.07 \times 10^{-4}$ of the electrical volume of the device (error reported for 1-sigma level). More importantly, droplets passing through different channels are mapped onto the same electrical volume due to the multimode measurement paradigm. Since water has a strong change in permittivity values in the 1-20GHz range, the empirically determined value of α is used when water replaces oil as in the microdroplet experiments. For the cell experiments biopolymers inside the cell effectively replace the water-rich media the channel, therefore the frequency-dependent factor of 1.6 is inverted in cell calculations.

S5. Microdroplet Measurements with a Second Device

More experiments were performed in a different device with thicker PDMS layer. To check the effect of channel position, the positions of microchannels were shifted in this device. The comparison of data obtained from the first and second devices are shown. Although the SNR for the second device is small and the channels are located at sub-optimal positions, clustering of the events on four sets are evident. Due to the lower SNR, clusters are broadened. For a few events where the second mode does not have a detectable signal, the event is marked on the df_1 axis. Moreover, the slopes of these clusters agree well with the relative positioning of the channels in the first and the second device.

Supporting Information for Towards Microwave Imaging of Cells

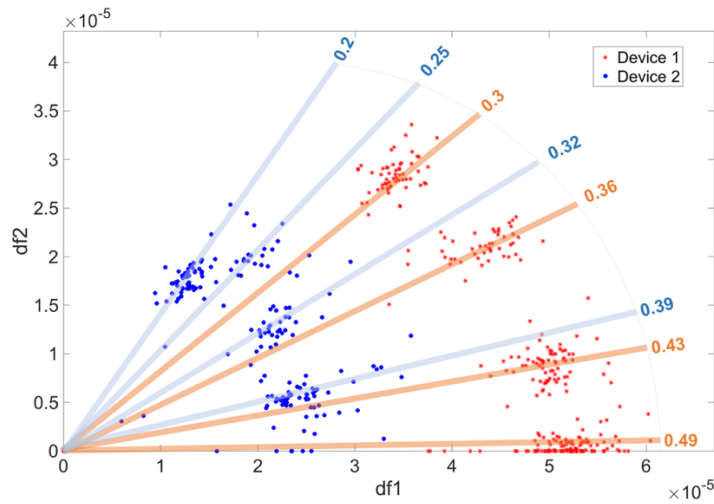


Figure 3: Scatter plot for events for two different devices. The second device has a larger electrical volume and its channels are shifted towards the edge.

S6. Experiments with a PCB Resonator with Holes

To implement the two mode detection principle, we also fabricated a microstripline resonator on a PCB. Small holes (of 1.2mm diameter) are drilled along the axis of the signal path of the microstripline to place analyte droplets. Glycerin was used as analyte due to its low vapor pressure and ease of handling. A volume of 1.8 μ L of glycerin was pipetted one by one into each of these holes. The resonance shifts before and after were measured using a spectrum analyzer with tracking generator capability. The experiments are repeated five times and the results are averaged to improve the signal to noise ration. The results are shown in Figure 5. Figure 5a shows the position detection calculated from the frequency shifts of both modes. The data points near the center of the resonator shows good agreement with the expected locations of the droplets. As the droplets are placed near the edges, the responsivity functions for each mode drop down: as a results, the signal-to-noise ratio of the measurements decrease and the measurements are less accurate. Moreover, these points are also more prone to non-idealities in boundary conditions. Nevertheless, the general trend is well established and it is clear that the center half of the resonators can be used for sensing applications.

Supporting Information for
Towards Microwave Imaging of Cells

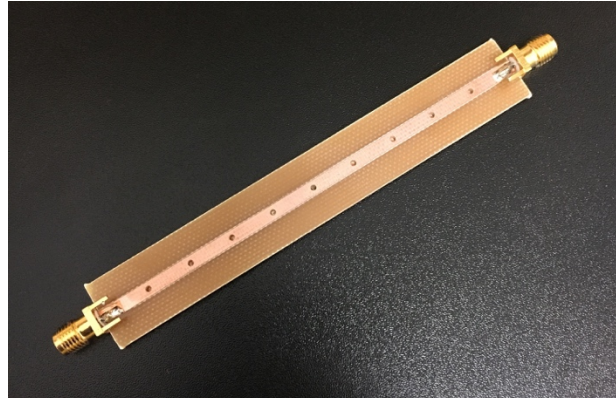


Figure 4: Microwave resonator based on a PCB was used to test the theory in an independent platform. Small holes are drilled at the center of the microstripline so that glycerin droplets can be deposited.

The electrical volume of the particle can also be determined as shown in Figure 5b.

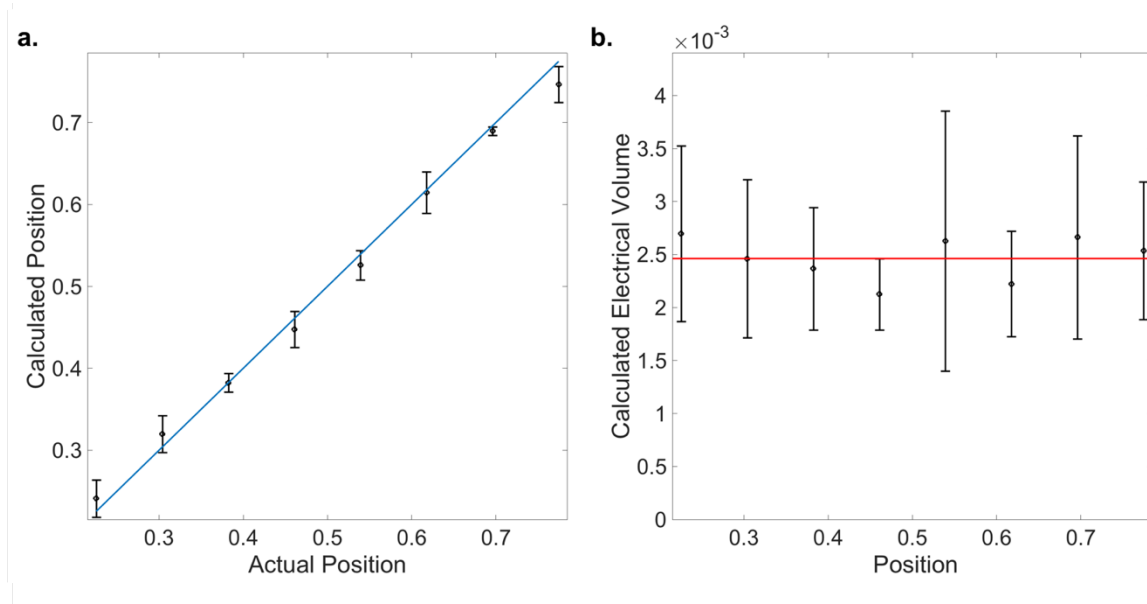


Figure 5: Experimental results for glycerin droplets deposited along a microstripline resonator. **a.** The normalized location of the droplets. Error bars show one-sigma standard deviation of the ensemble along each direction. **b.** The excess electrical volume of the droplet, as a portion of the total electrical volume of the resonator. Mean value for all measurements are shown in red, error bars are the one-sigma standard deviation of the ensemble along each direction.

S7. FEM Simulations

Microstrip based microwave sensor is modeled on COMSOL environment as follows. Substrate of the microstrip transmission line is chosen to be glass ($\epsilon_r = 4.2$) of 0.6mm height, 3mm width and 50mm length. Since the transmission length is small, conduction and impedance losses are negligible. Upper conductor and ground plane are defined by using perfect electric conductor boundary condition (width of the upper conductor is 1mm). To realize the $\lambda/2$ shorted transmission line resonators, a uniform rectangular lumped port boundary condition with excitation is defined on one end of the microstrip (lumped port on COMSOL is an approximation of the coaxial cable). On the other end we defined a rectangular area same as the previously defined lumped port's area, as perfect electric boundary condition which is in touch with upper conductor and ground plane so that the microstrip is shorted on one end. To operate in the most uniform Electrical field within the cross-section of the channel, sensing line is aligned with the upper conductor. A cylindrical microchannel of 100micron diameter is defined and its lateral axis is aligned with the central axis of the upper conductor. The carrier fluid is chosen as water. Sample particles are defined as 20micron sided cubes and placed within the microchannel. Material choice for the particles is oil of relative permittivity 2.5 which is close to the substrate material choice of glass. Microstrip transmission line is surrounded with an air box. The outer faces of the air box are defined as scattering boundary condition to eliminate/minimize the interference of the reflected waves. To get the most accurate results, we used the highest mesh option of extremely high mesh on our model and run the simulations on a supercomputer. In this mesh option, the smallest element size turned out to be 90 microns and resulted in a DOF number of 2.5 millions. Since the smallest change in meshing can reflect itself as a frequency shift, we run the simulations for each position twice and hold the meshing the same. The defined particle volume is filled once with a carrier fluid ($\epsilon_{r,water} = 78.3$), once with a material of interest ($\epsilon_{r,oil} = 2.5$). In this way, frequency shift caused by the presence of a particle in a continuous flow, is obtained as a snapshot of the flow.

Supporting Information for Towards Microwave Imaging of Cells

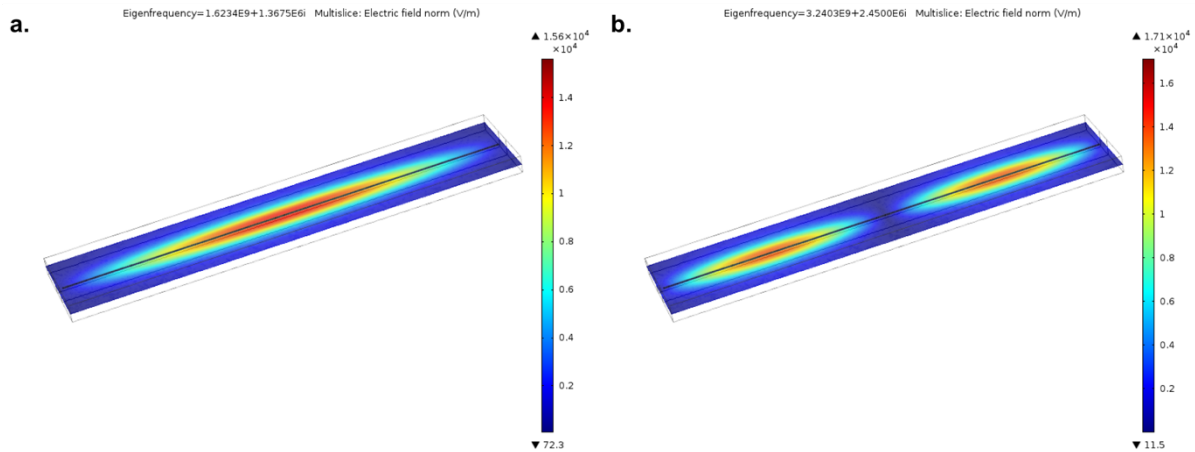


Figure 6: Snapshots for the first (a) and the second (b) modes in the COMSOL simulation. Shown here is the norm of the Electrical field. Channel structure is visible in the middle of the device.

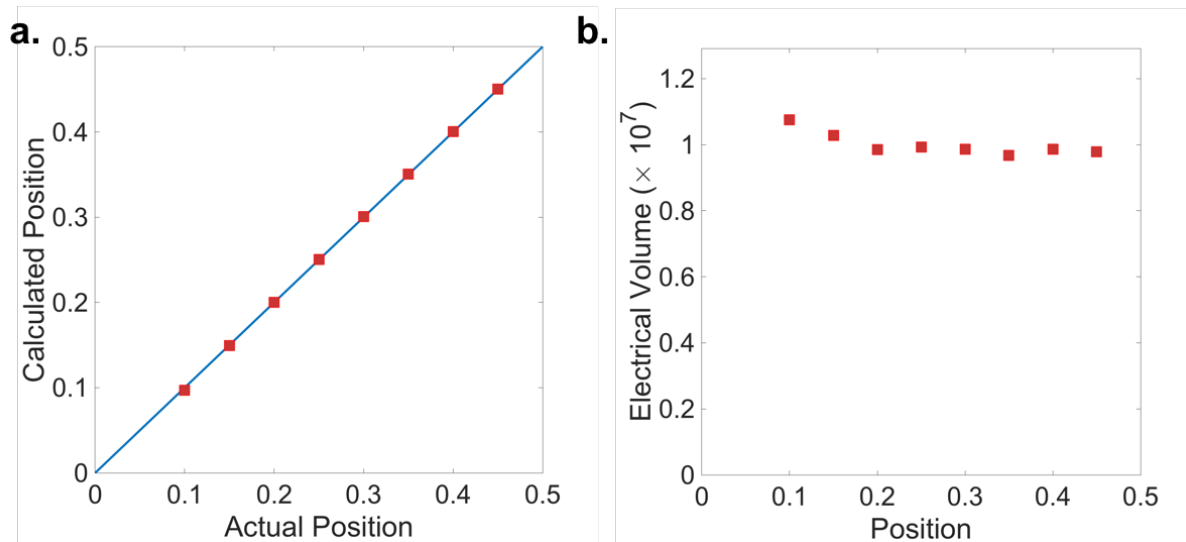


Figure 7: **a.** Simulation results for obtaining the location of a particle using two modes. **b.** Simulation results for obtaining the electrical volume of a particle using two modes.

References for the Supplementary Information Section

- 1 Pozar, D. M. *Microwave engineering*. (John Wiley & Sons, 2009).
- 2 Hanay, M. S. *et al.* Inertial imaging with nanomechanical systems. *Nature nanotechnology* **10**, 339-344 (2015).
- 3 Nikolic-Jaric, M. *et al.* Microwave frequency sensor for detection of biological cells in microfluidic channels. *Biomicrofluidics* **3**, 034103 (2009).
- 4 Hanay, M. S. *et al.* Single-protein nanomechanical mass spectrometry in real time. *Nature Nanotechnology* **7**, 602-608, doi:10.1038/nnano.2012.119 (2012).